Simulations of experimental conductance spectra of $YBa_2Cu_3O_y$ junctions: Role of a long *d*-wave decay length and a small *is* component in the pair potential near the interface

I. Lubimova and G. Koren
Physics Department, Technion—Israel Institute of Technology, Haifa 32000, Israel
(Received 14 May 2003; revised manuscript received 25 September 2003; published 31 December 2003)

Experimental conductance spectra of superconductor–normal metal–superconductor and superconductor-insulator-superconductor junctions, were simulated by an extended BTK model, where S is either a *d*-wave or $d+is$-wave superconductor. The model assumes a pure *d* wave in the bulk and coexistence of *d* and *is* near the interface. This implies that the bulk *d*-wave order parameter decays spatially near the interface with a typical ''decay length.'' We found that a relatively large decay length of the order of $10\xi_0-20\xi_0$ together with a small *is* component, can explain many peculiarities of the experimental conductance spectra. The good agreement of the simulation results with the experimental data, supports a scenario in which the experimentally observed *is* component is a surface property of the order parameter in the high-temperature superconductors.

DOI: 10.1103/PhysRevB.68.224519 PACS number(s): 74.20.Rp, 74.50.+r, 74.72.Bk

I. INTRODUCTION

An open question in the study of experimental conductance spectra of high-T_c junctions is whether the observed *is* (or id_{xy}) component of the order parameter[1–4] is a bulk or a surface property. Simple simulation results of these spectra assuming constant $d_{x^2-y^2}$ and *is* values throughout the bulk of the superconductor, yielded reasonable fits to the data of normal metal–insulator–superconductor (NIS) junctions in the tunneling regime,[3] but failed miserably to describe the data of superconductor–normal metal–superconductor (SNS) junctions over a wide range of energies.[4] Since bulk measurements such as thermal conductivity and specific heat in the high-T_c superconductors are consistent with a pure *d*-wave scenario without any *s*-wave component,[5,6] we made an effort in the present study to use a more realistic model for the simulation of the observed conductance spectra. In this model, a pure *d*-wave order parameter exists in the bulk, while a small *is* component, coexisting with the dominant *d* component, appears only near the interface. It turns out that this model can fit very well the observed SNS data over a wide energy range, and this seems to support a scenario in which the appearance of the *is* component occurs mostly near the interface.

Next we discuss how the special properties of d-wave superconductivity affect the different types of conductance spectra.[7,8] A large number of these studies deal with NIS or superconductor-insulator-superconductor (SIS) junctions in the tunneling limit where the effective Blonder-Tinkham-Vlapwijk (BTK) barrier strength

$$Z=\frac{mH}{\hbar^2 k_F} \tag{1}$$

is larger than ~ 1 (strong barrier).[9] Here H is the amplitude of the δ-function barrier at the interface. From a theoretical point of view, the tunneling limit is simpler to treat because in this limit of weak coupling between the electrodes, one can consider the electrodes as almost independent entities. More specifically, one can assume that the spatial changes of the superconducting order parameter, arising from the presence of a surface, occur only in a very small distance from the interface inside the superconductor. Thus, to a first-order approximation these changes are often ignored. Conductance spectra of NIS junctions where S is a *d*-wave superconductor, are characterized by a zero bias conductance peak (ZBCP) in the node direction, and by a gap in the antinode (main axis or lobe) direction. Theoretical calculations of low-transparency junctions reproduce these features quite well, also in the simpler case when a spatially independent pair potential is taken into account.[10] The ZBCP is a manifestation of zero-energy bound states of quasiparticles near the interface. The appearance of these bound states along the node direction of a *d*-wave superconductor results from the sign change of the energy gap $\Delta(\varphi_+)=-\Delta(\varphi_-)$, where $\varphi_\pm$ are the angles between the wave vector of the incoming or scattered quasiparticle and the normal to the interface, and $\varphi_+=\pi-\varphi_-$.

Theoretical calculations of the conductance spectra of junctions with a weak barrier are more problematic. The problem arises from the strong mutual dependence of the pair potential on both sides of the NS interface. This is in contrast to the strong barrier case, where the two electrodes are almost decoupled. Thus, in order to obtain an explicit form of the spatial dependence of the pair potential, a complete knowledge of the quasiclassical Green function is necessary, not only in the S side but also in the N side of the junction. Therefore, a proximity effect must be directly included in the calculations. There is no consensus on the peculiarities of the proximity effect in junctions with anisotropic superconductors at the present time. The penetration length of the order parameter into the N (normal metal) side and its symmetry there, depend sensitively on the specific properties of the normal metal.[11–15] Recently, it was found that even ferromagnetic or antiferromagnetic metals in NS junctions have a long-range proximity effect under certain conditions,[16–18] and this is in contrast to the predictions of certain theories.[19] For the 123-family of superconductors, the length scale of the proximity effect in the N side depends significantly on the oxygen-doping level of the S side. This results from the fact that in underdoped yttrium barium copper oxide (YBCO) T_c is reduced compared to optimal doping, and the value of the coherence length is increased. *A*

priori the proximity interaction between the two electrodes should depend strongly on the barrier strength. But as was shown previously,[20–22] the effect of the barrier is not always so evident, and even a barrier of finite strength is not always effective in reducing the conductance of the junctions. In particular, in NS junctions with similar materials and similar density of states (DOS) on both sides, the influence of a barrier is suppressed significantly. This occurs when both electrodes are made of differently doped cuprate compounds. According to Deutscher and De Gennes,[23] in such cases the amplitude of the order parameter in the normal side near the interface can reach a value close to that in the superconductor, and there is almost no discontinuity or jump at the interface. Therefore, in this type of junction the diffusion of pairs from the superconductor into the metal is almost unaffected by the barrier, and the decay distance of pairs in the normal phase may be anomalously large.

YBCO has a short coherence length $\xi_0=\hbar v_F/\Delta_0$ of about 10–30 Å where Δ_0 is the bulk value of the *d*-wave pair potential.[24] In spite of this fact, it follows from the above discussion that in studies of NS junctions with similar cuprates one should examine a wide range of decay lengths in S and proximity lengths in N. To clarify this different length scales dependence, we decided to calculate the corresponding conductance spectra in a phenomenological way. This is justified in view of the complexity of the problem that already for conventional superconductors is not trivial.[25] We did not develop a new model for self-consistent calculations of the pair potential in proximity systems. Instead, we assumed reasonable pair potential shapes, and calculated the resulting conductance spectra. From the results we were able to identify which of the peculiarities of the pair potential had the most significant effect on the conductance spectra, and what form of its spatial dependence leads to the best fit of the experimental data.

II. RESULTS AND DISCUSSION

A. The model

We have calculated numerically the conductance spectra of a normal metal (N)–*d*-wave superconductor (S) junction as a function of applied voltage using the basic model developed by Tanaka and Kashiwaya.[7] According to their theory, the conductance is given by

$$\sigma(eV)=\frac{\int_{-\pi/2}^{\pi/2}\int_{-\infty}^{\infty}\sigma_S(E,\varphi)\left(-\frac{\partial f(E+eV)}{\partial E}\right)\sigma_N(\varphi)\cos\varphi\, d\varphi\, dE}{\int_{-\pi/2}^{\pi/2}\sigma_N(\varphi)\cos\varphi\, d\varphi}, \tag{2}$$

where the integrations are over the angles between the trajectory of the incoming quasiparticle and the normal to the interface of the junction, and the energy. The normal metal conductance σ_N characterizes the transparency of the junction and is given by

$$\sigma_N=\frac{4\cos^2\varphi}{4\cos^2\varphi+Z^2}, \tag{3}$$

where Z is the effective barrier strength as given by Eq. (1). $f(E)$ in Eq. (2) is the Fermi distribution function at temperature *T*. The function σ_S in Eq. (2) represents an extension of the standard BTK expression for the conductance[9]

$$\sigma_S=1-|b|^2+|a|^2, \tag{4}$$

to the case of spatial dependent order parameter. In Eq. (4), *b* and *a* are the coefficients of the normal and Andreev reflections, respectively. In the simple BTK model, the reflection coefficients are expressed in terms of the functions $\Gamma_{\pm}(E,\varphi)$ in the following way:

$$\frac{\sigma_S}{\sigma_N}=\frac{1+\sigma_N|\Gamma_+|^2+(\sigma_N-1)|\Gamma_+\Gamma_-|^2}{|1+(\sigma_N-1)\Gamma_+\Gamma_-|^2}. \tag{5}$$

The $\Gamma_{\pm}$ in this equation are functions of the energy *E* and angle φ only, since the pair potential is assumed to be spatially constant. In the present study however, we use the extended BTK model which takes into account the spatial dependence of the superconducting pair potential. Following Kashiwaya and Tanaka,[7] we calculated the $\Gamma_{\pm}$ values at the interface by solving a set of Riccati type equations [Eqs. (3.50)–(3.52) in Ref. 7] in which the spatial dependent pair potentials $\Delta_{\pm}(\varphi,x)$ appear as coefficients (*x* is the distance from the interface in S).

In our simulations we have chosen the following functions to represent the spatial dependence of the pair potential of the dominant $d_{x^2-y^2}$ and subdominant *s* components of the order parameter

$$\frac{\Delta_{d_{x^2-y^2}}(\zeta)}{\Delta_0}=\tanh((\zeta+k_1)*k_2), \tag{6}$$

and

$$\frac{\Delta_s(\zeta)}{\Delta_0}=k_3\exp(-k_4^*\zeta^2), \tag{7}$$

where $\zeta=x/\xi_0$ is a dimensionless length (see Fig. 1). The superconductor occupies $x\geqslant 0$ and the interface is exactly at $x=0$. Here the k_i $(i=1\ldots4)$ are dimensionless parameters

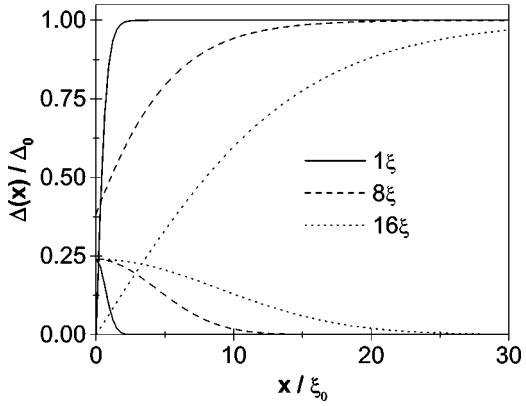

FIG. 1. Typical spatial dependencies of the normalized *d*-wave and *s*-wave pair potentials with different decay lengths near the interface used in our simulations. Δ_0 is the energy gap value in the bulk of the superconductor.

which depend on the junction orientation relative to the crystalline axis. The modeling functions in Eqs. (6) and (7), satisfy the main boundary conditions on both component of the pair potential ($\Delta_{d_{x^2-y^2}} \rightarrow \Delta_0$ and $\Delta_s \rightarrow 0$ as $x \rightarrow \infty$), and are consistent with the self-consistent model results.[27,26] Moreover, we note that the fine details of the spatial dependence of the pair potential is not essential, as it does not affect the resulting spectra in any major way. In order to confirm this statement, we examined different possible functions by replacing, for instance, $\tanh(\zeta)$ with $1-\exp(-\zeta)$. Results of these calculations show that such changes lead only to minor changes in the energies of the high-order bound states in the conductance spectra. We found out that the most important parameters of the pair potential shape which affect the conductance spectra are the maximal amplitude of the subdominant component [the k_3 coefficient in Eq. (7)] and the quasiparticle decay length, which represents the characteristic length scale over which the pair potential varies spatially near the interface [governed by k_1, k_2, and k_4 in Eqs. (6) and (7)].

In all our calculations we have taken into account the thermal smearing factor which is due to the finite (low) temperature, and the finite lifetime broadening of the quasiparticles at the Fermi surface. It is a well-known fact from the theory of Fermi liquids[28] that the inverse lifetime of the quasiparticles is proportional to E^2. In real superconductors, there are some quasiparticle relaxation processes which include electron-electron and electron-phonon interactions, which modify this simple square law dependence. Kaplan *et al.*[29] showed that the general dependence of such relaxation rates can have a very complicated dependence on energy which is unique for each material. Dynes *et al.*, however, used successfully a constant lifetime broadening in the theoretical fits of their measured conductance spectra in low-T_c SIS junctions.[30] Such approximation indeed works well for fitting of the experimental spectra in isotropic superconductors and in the low-transparency limit. In this case, $\Delta(x) \approx$ constant, the conductance is proportional to the quasiparticle density of states, and this has strong sharp peaks at $E = \pm \Delta_0$. The addition of lifetime broadening as a small imaginary part to the energy allows one to avoid divergence at the peak energies and does not produce any essential change in other regions. Our attempt, however, to apply this method to high-transparency spectra was unsuccessful. We attribute this to the appearance of additional bound states due to a significant increase in the decay length (see below). It is thus clear that in such cases, taking into account the energy dependence of the lifetime broadening is essential. In our calculations we used a fourth-degree polynomial approximation for this dependence:

$$\Gamma(E) = \gamma_1 E^2 + \gamma_2 E^3 + \gamma_3 E^4, \tag{8}$$

where the coefficients $\gamma_i \leqslant 1$ (in units of Δ_0) were chosen in order to obtain the best fit to the experimental conductance spectra. It should be noted, however, that the first term in Eq. (8) is sufficient to reproduce most of the conductance spectra features, while the last two terms improve the fits only at high energies of $E \geqslant 0.5\Delta_0$. Generally, the function Γ is added as an imaginary part to the energy in the expression for the DOS.[30,7] In our calculations, however, the equivalent of the DOS is the function σ_S of Eq. (2). Since we obtain σ_S by solving two coupled differential equations in which the energy is a parameter, we could not just add the $i\Gamma$ term to E directly. The fact that the boundary conditions of these equations include nonlinear terms in E is an additional complication. We therefore calculated σ_S first without any broadening term, and then added the broadening numerically by a convolution of the obtained $\sigma_S(E)$ function for each angle φ, with a Lorentzian distribution function

$$L(E) = \frac{1}{\pi} \frac{\Gamma(E)}{(E-E_0)^2 + \Gamma^2(E)} \tag{9}$$

of width $\Gamma(E)$.

B. Bound states in a pure *d*-wave symmetry

We now discuss the effect of bound states on the conductance spectra in the case of a pure *d*-wave symmetry of the order parameter without any subdominant component. In principle, two basically different cases of the node ($\alpha = \pi/4$) and antinode ($\alpha = 0$) orientations should be considered. α is the angle between the lobe direction of the $d_{x^2-y^2}$-wave order parameter and the normal to the interface. As we shall see in the following the presence of bound states affect the conductance spectra significantly in both directions, but in the present section we shall focus on the node direction. In this direction, a ZBCP exists independently of the values of the coefficients k_1 and k_2 in Eq. (6), and the effective barrier strength Z. Nevertheless, by varying k_1 and k_2 in Eq. (6), the shape of the calculated conductance spectra changes. Decreasing their values, leads to an increased suppression of the order parameter at the interface and an increased decay length. As a consequence, additional quasiparticle bound states are created.[31,26] These new bound states are formed in a potential well defined by the interface on one side and the growing d-wave pair potential toward the bulk value on the other side. They manifest themselves as additional peaks in the function $\sigma_S(E)$ versus E. Their number

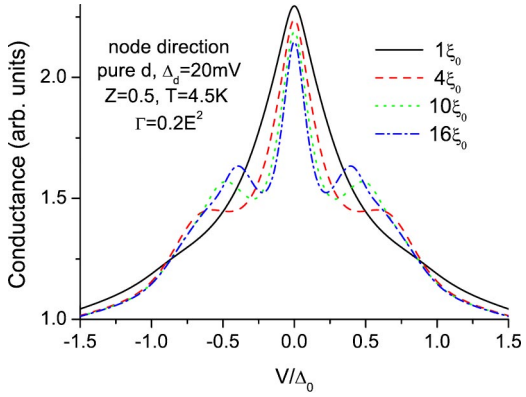

FIG. 2. (Color online) Simulations of normalized conductance spectra of a high-transparency SN junction with $Z=0.5$ along the node direction for a pure *d*-wave symmetry of the pair potential. Different curves correspond to different values of the decay length.

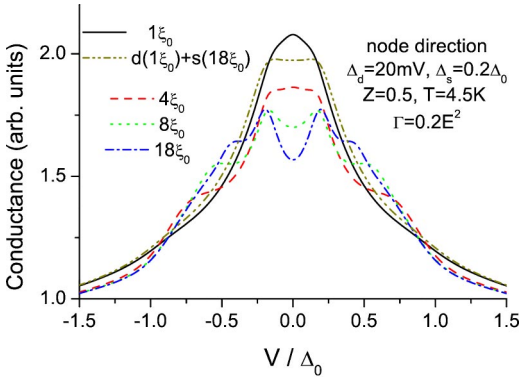

FIG. 3. (Color online) Theoretical curves of normalized conductance spectra of a high-transparency NS junction along the node direction using a $d+is$ symmetry of the pair potential. In each curve the decay length of both components of the pair potential is the same, except for the dash-double-dotted line where the decay length of the *d*-wave component is ξ_0 while that of the *s*-wave component is $18\xi_0$.

and energies vary for different angles φ, and according to Matsumoto and Shiba,[26] their energies are given by

$$E_n = \pm \Delta_0 |\sin(2\varphi)| \sqrt{\frac{n}{r}\left(2-\frac{n}{r}\right)}, \tag{10}$$

where n is an integer,

$$r = \frac{2|\sin(2\varphi)|}{k_2}, \tag{11}$$

and $0<n<r$. k_2 in Eq. (11) is different from zero since a $k_2=0$ in Eq. (6) would yield $\Delta \equiv 0$, which means that no superconductivity exists. The number of bound states is determined by r. The larger the value of r the larger the number of these states. Equation (11) does not give the dependence of r on k_1, because in Ref. 26 only the special case of a superconductor-vacuum interface is considered ($Z\to\infty$). Therefore in Ref. 26, k_1 is always zero in the node direction. It is however clear from Eq. (6) that with increasing k_1 the potential well is filled up, the spatial dependence of Δ approaches that of a step function, and the bound states disappear. Thus, in the general case of arbitrary Z and α, the number of bound states is proportional to the depth of the potential well. This depends on both coefficients k_1 and k_2, and yields a more general expression for r as follows:

$$r = \frac{2|\sin(2\varphi)|}{k_2}[1-\tanh(k_1 k_2)]. \tag{12}$$

Equation (12) shows that while we consider quasiparticles within a narrow cone around $\varphi=0$ (just as in SIN junctions), bound states will play a less significant role in the conductance (if the cone angle $\varphi\to 0$ then there are no bound states since $r\to 0$). In the weak barrier limit though, a broad cone of about $-\pi/2<\varphi<\pi/2$ should be used, and the influence of bound states on the conductance spectra becomes substantial as seen in Fig. 2. On each curve of this figure only two symmetrical maxima besides the ZBCP are present. The curves in Fig. 2, however, show the $\sigma(eV)$ dependence on V and not the $\sigma_S(E)$ dependence on E. In the latter for each value of φ a different number of additional maxima exist. After integration of σ_S over all angles φ, only two main peaks versus energy are left which contribute to the resulting maxima E_{pd} in $\sigma(eV)$ as seen in Fig. 2. These side band peaks are the second-most prominent features in the spectra. With increasing r, the voltage of these peaks shifts to low bias. Because of this, after the integration in Eq. (2) the ZBCP becomes somewhat smaller and its width decreases. It is important to note that in spite of the shift of additional maxima towards zero bias with increasing decay length of the pair potential, they cannot annihilate the ZBCP, since the zero-energy bound state is robust and exists for *all* values of φ, while the other bound states are not. Therefore, by changing the parameters k_1 and k_2 we cannot obtain splitting of the ZBCP in the node direction in the pure *d*-wave case.

C. Node results for $d+is$ symmetry

Splitting of the ZBCP along the node direction was, however, measured in SNS junctions.[4] In order to fit this data, it was necessary to add a subdominant component to order parameter with a different symmetry. Because of previous results,[1,2] we have chosen for this purpose to add an imaginary *s*-wave component to the pair potential. Now the form of the resulting order parameter depends on all four coefficient k_1, k_2, k_3, and k_4. Our calculation results along the node direction and with a small Z value are shown in Fig. 3. The main conclusion from this figure is that the subdominant component can not essentially influence the conductance spectra as long as the decay length of the dominant *d*-wave component is $\sim\xi_0$. This behavior is different from that observed in the strong barrier limit, where a small decay length for both components is enough for obtaining splitting of the ZBCP (not shown). Tanuma *et al.* have obtained no subdominant component for low values of Z ($Z\sim 1$),[27] even though their Z value is defined as twice the BTK Z value that we use here. In addition, the order parameter that they obtained, almost always had a decay length of order $\sim\xi_0$. However, when we repeated their self-consistent calculations

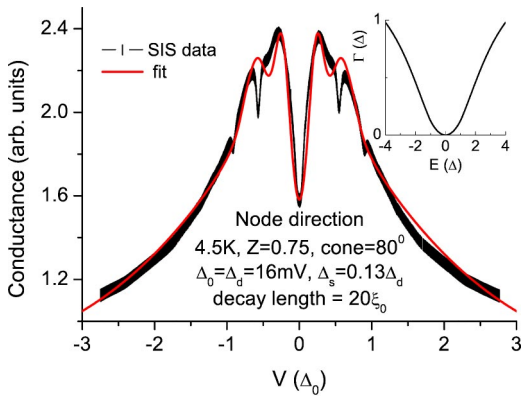

FIG. 4. (Color online) Measured normalized conductance spectra of a high-transparency $YBa_2Cu_3O_{6+x}/YBa_2Fe_{0.45}Cu_{2.55}O_{6+x}/YBa_2Cu_3O_{6+x}$ junction along the node direction (symbols) together with a best-fit simulation (line). The broadening Γ vs E is given in the inset.

for high-transparency junctions, we could find cases (when $T_{cs}=0.5T_{cd}$ for instance) in which the *s* component did exist and had a long penetration length of the order of $10\xi_0$ into the bulk. Moreover, in their self-consistent calculations of the order parameter they did not take into account the proximity effect. Therefore, the absence of a subdominant component in the results of Tanuma *et al.* for weak barriers is not contradictory to our results. As can be seen in Fig. 3, we obtain the splitting effect by the *s*-wave component only when d-wave decay lengths longer than a few ξ_0 are used.

A subdominant *is* component splits the ZBCP into two peaks, whose energy $|E_{ps}|$ depends on the values of k_3 and k_4 in Eq. (7). There is no exact analytic formula for this dependence, but numerical calculations yield an approximate relation

$$|E_{ps}| \sim c_1 k_3 \exp(-c_2 k_4) \quad \text{for} \quad k_3 < \Delta_0, \tag{13}$$

where c_1 and c_2 are constants which depend on *Z*. When two components of the order parameter coexist, the conductance spectra is a superposition of contributions containing the bound states of both. These bound states can annihilate one another unless the value of E_{ps} is close to the energy E_{pd} of the bound states of the dominant component. It thus follows that the smaller the *s*-wave component, the larger the required decay length of the *d* component, which is needed in order to obtain a clear splitting.

A simulation of a the conductance spectra fitting our previous experimental data along the node direction is given in Fig. 4. The original data was obtained for SNS junctions.[4] Since no theoretical model is available at the present time for the calculation of the conductance of SNS junctions which takes into account the finite decay length of the pair potential at the interface, we used as a first approximation the SN model discussed here, but with a renormalized energy scale to fit the SNS data. This renormalization was simply done by doubling the energy scale in the SN calculations (multiplying it by a factor of 2). We can thus compare the modified SN simulation results with the measured SNS data on the same energy scale of E/Δ_0. Coexistence of both *d* and *is* components of the order parameter near the interface had to be assumed in order to fit the data. The good agreement between theory and experiment indicates that relatively large decay lengths of the order of $20\xi_0$ of the d-wave pair potential are actually present near the interface of real junctions. It should be stress here that although many free parameters appear in Eqs. (6)–(8), in the actual simulation their number was kept to a minimum. Since the fits were quite insensitive to k_1, we always used $k_1=0$. We also assumed equal decay lengths for the *d* and *s*-wave components $n_d\xi_0=n_s\xi_0=n\xi_0$, by the use of the relation $1-\tanh(k_2 n_d)=\exp(-k_4 n_s^2)=0.2$. Thus, the number of adjustable parameters k_1, k_2, and k_4 is reduced from three to one ($n\xi_0$). Moreover, good simulation spectra were obtained at energies of up to $E\approx 0.5\Delta_0$ by the use of only the first term in Eq. (8) ($\gamma_1 \neq 0$ and $\gamma_2=\gamma_3=0$). Therefore, we could basically describe the main features of the measured spectra by using only three adjustable parameters, namely, the decay length $n\xi_0$, the size of the *s*-wave component at the interface k_3, and the Landau broadening coefficient γ_1. Considering the complexity of the problem, this is quite remarkable. An important open question that the present simulation result helps to resolve is whether the observed *s* component of the order parameter in the high temperature superconductors is a surface or a bulk property. Since the present model clearly assumes that the *s*-wave component exists only near the interface, the good agreement between the simulation result and the experimental data as shown in Fig. 4 supports the notion that the *s* component is a surface phenomenon.

D. Lobe results for mostly *d*-wave symmetry

We now turn to junctions along the antinode direction. This direction is characterized in the tunneling regime by a ''V'' shaped conductance spectra with a minimum at zero bias whose depth is a function of the barrier strength *Z*. For a low-transparency barrier $\sigma(E=0)\sim 0$, but as *Z* decreases this value increases. For weak barriers (small *Z*) the conductance is controlled mostly by Andreev reflections, and $\sigma(E=0)$ reaches a value of 2 when $b=0$ and $a=1$ in Eq. (4). Again, we varied the values of the coefficients k_i ($i=1\ldots 4$) in order to study the influence of the order parameter near the interface on the conductance spectra. Qualitatively, all our previous reasoning remain valid. Decreasing k_1 and k_2 leads to the appearance of bound states which are seen as new maxima in the simulated conductance curves. Similar to the results along the node direction, we find that with increasing decay length of the *d*-wave pair potential, the bound-states appear at lower bias. But they never occur at zero bias, where the conductance minimum persists up to very low *Z* values. Figure 5 shows simulations of conductance spectra for a weak barrier of $Z=0.5$ along the (100) direction for different values of the coefficient k_2 while $k_1=0$. The main feature of these spectra is that the peaks at the subgap energies increase with decreasing k_2 (increasing decay length). Moreover, addition of a small subdominant s-wave component to the *d*-wave order parameter when a large decay length is used, does not practically change the form of the conductance spectra (the solid and dotted curves

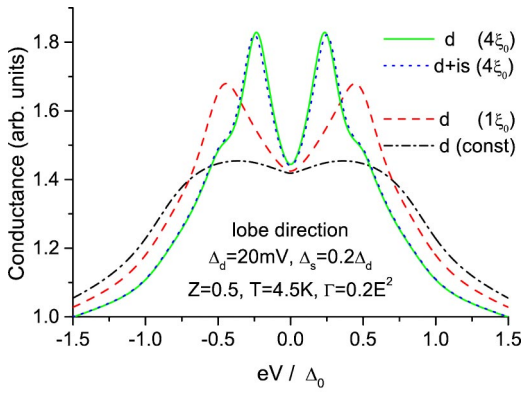

FIG. 5. (Color online) Calculated normalized conductance spectra of a high-transparency SN junctions with Z=0.5 along the lobe direction. All curves were obtained by the use of a pure *d*-wave symmetry of the pair potential with various decay length, except for the dotted line where a $d+is$ symmetry was used.

in Fig. 5 are almost indistinguishable). This leads to an important conclusion that the conductance along the (100) direction in high-transparency junction with a long-range proximity effect is basically insensitive to the presence of possible subdominant components of order parameter.

Figure 6 shows experimental conductance spectra of a low-transparency junction along the (100) direction,[4] together with a best-fit simulation for this case. The energy scale of the SIN simulation was renormalized to the equivalent SIS scale of the experiment as before (was multiplied by a factor of 2). The low transparency is a result of a large normal resistance R_N which is found in the experiment for the (100) orientation. The roughness of the interface in this type of junction was found to be smaller than the coherence length ξ_0, thus no faceting can lead to the low transparency. Twinning, however, can cause different R_N values in different directions. We found out that a pure *d*-wave order parameter neither with a small nor with large decay length can fit our data well, especially not at low bias (see the dash and

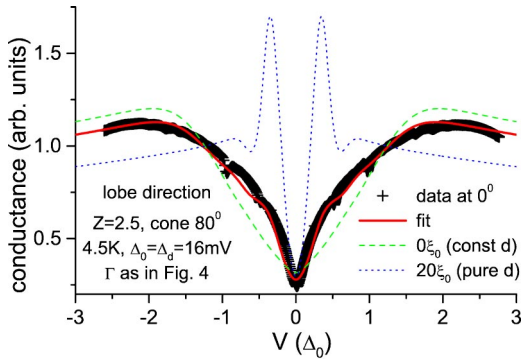

FIG. 6. (Color online) Measured normalized conductance spectra along the lobe direction (symbols) of a low-transparency junction of $YBa_2Cu_3O_{6+x}/YBa_2Fe_{0.45}Cu_{2.55}O_{6+x}/YBa_2Cu_3O_{6+x}$ together with a best theoretical fit (solid line). The energy dependent lifetime broadening $\Gamma(E)$ is the same as that in Fig. 4. Also shown are the conductance contributions of a constant *d* wave (dash line) and a *d* wave with $20\xi_0$ decay length (dotted line).

dotted curves in Fig. 6). It turned out that the contribution of bound states is essential in order to describe correctly the low-energy dependence of the experimental conductance spectra. A typical contribution of bound states is shown in Fig. 6 by the dotted curve for a $20\xi_0$ decay length. For the best fit in this figure we used an *ad hoc* superposition of mainly a constant *d*-wave component (76%), and the additional contributions from three longer decay lengths of $3\xi_0$, $10\xi_0$, and $20\xi_0$ (8% of each), and found a remarkable agreement between the simulation and the experimental data (the solid line in Fig. 6). The fact that we had to use such a superposition means that in reality, at least in the lobe direction, there is some nonuniformity in the values of the decay length over the junction cross section. This can be due to the twinning mentioned above, to a nonuniform oxygen distribution or to some other disturbances. We note that in grain boundary junctions a nonuniform distribution of different barrier widths was found,[32] which in a way is similar to the decay length distribution observed here. As was discussed before in connection with the simulation results of Fig. 4, here again the basic results of the simulation in Fig. 6 could be obtained by the use of only three adjustable parameters. Although we added two free parameters (the two new decay lengths), we also removed two adjustable parameters (the size of the *s* component $k_3=0$, and the γ_i, since we used the same broadening function as found in Fig. 4). We therefore kept the number of adjustable parameters to a minimum, which should give further support to the reliability of our simulation results.

E. Summary

In the following we summarize the main properties of SN and SIN junctions resulting from our simulations:

(i) For a pure *d*-wave superconductor in the node-direction, large decay lengths of the order parameter near the interface lead to additional peaks in the conductance spectra at subgap biases. The peak energies shift to lower bias with increasing decay length of the order parameter, while the ZBCP amplitude and its width decrease.

(ii) In order to obtain a well-defined splitting of ZBCP in the conductance spectra along the node direction as seen in the experiment, one has to add a small subdominant is component to the order parameter, and keep a long decay length.

(iii) In contrast, while using a pure *d* wave with a large decay length in high-transparency junctions along the lobe direction, the gap peaks in the conductance move to lower energies and this looks like splitting of the broad Andreev-enhanced conductance regime at $E \lesssim \Delta_0$.

(iv) The energy dependence of the quasiparticles lifetime broadening has to be taken into account in the simulations of the conductance spectra.

(v) The fact that a long decay length in the superconductor had to be used in order to obtain good agreement between the theoretical simulations and the measured conductance spectra gives further support to the notion that a long-range proximity effect exists in the cuprates.

III. CONCLUSIONS

In the present study we investigated how the spatial dependence of the order parameter near the interface of junctions affects the resulting conductance spectra. We found that the decay length of the *d*-wave pair potential is the most significant parameter affecting the spectra. More specifically, for high-transparency junctions along the node direction, the use of a long decay length of the order of $10\xi_0-20\xi_0$ yields a splitting of the ZBCP, provided an additional small is component exists near the interface. If in contrast a $\sim\xi_0$ decay length is used, no such splitting develops in the simulations, and this is in contradiction to experimental observations. For low-transparency junction along the main lobe direction, a small decay length of the order of $\sim\xi_0$ could not describe the data neither with a pure *d*-wave nor with a $d+is$ order parameter. Only when a distribution of decay lengths between $0\xi_0$ and $20\xi_0$ was assumed, small contributions from additional bound states led to a good fit of the experimental data. Another important parameter that affects the conductance spectra strongly is the quasiparticles lifetime broadening and its nontrivial energy dependence $\Gamma(E)$. We actually modified its basic Fermi-liquid E^2 dependence to fit the experimental data along the node direction, and then used it successfully without any further changes to fit the lobe data. We note that a long decay length in the S side is consistent with a reversed proximity effect in high-transparency SN junctions, and the low T_c of the is component. An important conclusion from the present simulation results is that the experimentally observed *s*-wave component in conductance spectra of the high-T_c superconductors is a surface phenomenon.

ACKNOWLEDGMENTS

This research was supported in part by the Israel Science Foundation, the Heinrich Hertz Minerva Center for HTSC, the Karl Stoll Chair in advanced materials, the Fund for the Promotion of Research at the Technion, and by the Center for Absorption in Science, The Ministry of Immigrant Absorption of the State of Israel.

[1] M. Covington, M. Aprili, E. Paraoanu, L.H. Greene, F. Xu, J. Zhu, and C.A. Mirkin, Phys. Rev. Lett. **79**, 277 (1997).
[2] R. Krupke and G. Deutscher, Phys. Rev. Lett. **83**, 4634 (1999).
[3] A. Sharoni, O. Millo, A. Kohen, Y. Dagan, R. Beck, G. Deutscher, and G. Koren, Phys. Rev. B **65**, 134526 (2002).
[4] G. Koren and N. Levy, Europhys. Lett. **59**, 121 (2002).
[5] M. Sutherland, D.G. Hawthorn, R.W. Hill, F. Ronning, S. Wakimoto, H. Zhang, C. Proust, E. Boaknin, C. Lupien, L. Taillefer, R. Liang, D.A. Bonn, W.N. Hardy, R. Gagnon, N.E. Hussey, T. Kimura, M. Nohara, and H. Takagi, Phys. Rev. B **67**, 174520 (2003).
[6] K.A. Moler, D.J. Baar, J.S. Urbach, R. Liang, W.N. Hardy, and A. Kapitulnik, Phys. Rev. Lett. **73**, 2744 (1994).
[7] S. Kashiwaya and Y. Tanaka, Rep. Prog. Phys. **63**, 1641 (2000), and references therein.
[8] C.C. Tsuei and J.R. Kirtley, Rev. Mod. Phys. **72**, 969 (2000).
[9] G.E. Blonder, M. Tinkham, and T.M. Klapwijk, Phys. Rev. B **25**, 4515 (1982).
[10] S. Kashiwaya, Y. Tanaka, M. Koyanagi, H. Takashima, and K. Kajimura, Phys. Rev. B **51**, 1350 (1995).
[11] Y. Ohashi, J. Phys. Soc. Jpn. **65**, 823 (1996).
[12] J.E. Sonier, J.H. Brewer, R.F. Kiefl, D.A. Bonn, S.R. Dunsiger, W.N. Hardy, Ruixing-Liang, W.A. MacFarlane, R.I. Miller, T.M. Riseman, D.R. Noakes, C.E. Stronach, and M.F. White Jr., Phys. Rev. Lett. **79**, 2875 (1997).
[13] R.S. Decca, H. Drew, E. Osquiguil, B. Mairov, and J. Guimpel, Phys. Rev. Lett. **85**, 3708 (2000).
[14] E. Polturak, O. Nesher, and G. Koren, Phys. Rev. B **59**, 6524 (1999).
[15] B. Pannetier and H. Courtois, J. Low Temp. Phys. **118**, 599 (2000).
[16] E. Demler, A.J. Berlinsky, C. Kallin, G.B. Arnold, and M.R. Beasley, Phys. Rev. Lett. **80**, 2917 (1998).
[17] F.S. Bergeret, A.F. Volkov, and K.B. Efetov, Physica C **367**, 107 (2002).
[18] A. Kadigrobov, R.I. Shekhter, and M. Jonson, Europhys. Lett. **54**, 394 (2001).
[19] E. Demler, G. Arnold, and M.R. Beasly, Phys. Rev. B **55**, 15174 (1997).
[20] A. Golubov and M.Y. Kupriyanov, Zh. Eksp. Teor. Fiz. **96**, 1420 (1989) [Sov. Phys. JETP **69**, 805 (1989)].
[21] B.J. van Wees, P. de Vries, P. Magnee, and T.M. Klapwijk, Phys. Rev. Lett. **69**, 510 (1992).
[22] M. Schechter, Y. Imry, and Y. Levinson, Phys. Rev. B **64**, 224513 (2001).
[23] G. Deutscher and P. G. de Gennes, in *Superconductivity*, edited by R. Parks (Marcel Dekker, New York, 1969), Vol. 2.
[24] Y. Ando and K. Segawa, Phys. Rev. Lett. **88**, 167005 (2002).
[25] K. Haltermann and O.T. Valls, Phys. Rev. B **66**, 224516 (2002).
[26] M. Matsumoto and H. Shiba, J. Phys. Soc. Jpn. **12**, 4867 (1995).
[27] Y. Tanuma, Y. Tanaka, and S. Kashiwaya, Phys. Rev. B **64**, 214519 (2001).
[28] D. Pines and Ph. Nozières, *The Theory of Quantum Liquids* (Benjamin, New York, 1966), Vol. 1.
[29] S.B. Kaplan, C.C. Chi, D.N. Langenberg, J.J. Chang, S. Jafarey, and D.J. Scalapino, Phys. Rev. B **14**, 4854 (1976).
[30] R.C. Dynes, V. Narayanamurti, and J.P. Garno, Phys. Rev. Lett. **41**, 1509 (1978).
[31] Yu.S. Barash, A.A. Svidzinsky, and H. Burkhardt, Phys. Rev. B **55**, 15282 (1997).
[32] H. Hilgenkamp and J. Mannhart, Rev. Mod. Phys. **74**, 485 (2002).